01 Jan 2005

Near-Field Intensity Correlations in Semicontinuous Metal-Dielectric Films

K. Seal

A. K. Sarychev

H. Noh

D. A. Genov

et. al. For a complete list of authors, see https://scholarsmine.mst.edu/phys_facwork/370

Recommended Citation

K. Seal et al., "Near-Field Intensity Correlations in Semicontinuous Metal-Dielectric Films," *Physical Review Letters*, American Physical Society (APS), Jan 2005.
The definitive version is available at https://doi.org/10.1103/PhysRevLett.94.226101

Near-Field Intensity Correlations in Semicontinuous Metal-Dielectric Films

K. Seal,[1] A. K. Sarychev,[2] H. Noh,[1] D. A. Genov,[3] A. Yamilov,[1] V. M. Shalaev,[3] Z. C. Ying,[4] and H. Cao[1]

[1]*Department of Physics and Astronomy, Northwestern University, Evanston, Illinois 60208, USA*
[2]*Ethertronics Inc., 9605 Scranton Road, Suite 850, San Diego, California 92121, USA*
[3]*School of Electrical and Computer Engineering, Purdue University, West Lafayette, Indiana 47907, USA*
[4]*National Institute of Standards and Technology, Gaithersburg, Maryland 20899, USA*

(Received 18 August 2004; published 8 June 2005)

Spatial intensity correlation functions are obtained from near-field scanning optical microscope measurements of semicontinuous metal-dielectric films. The concentration of metal particles on a dielectric surface is varied over a wide range to control the scattering strength. At low and high metal coverages where scattering is weak, the intensity correlation functions exhibit oscillations in the direction of incident light due to excitation of propagating surface waves. In the intermediate regime of metal concentration, the oscillatory behavior is replaced by a monotonic decay as a result of strong scattering and anomalous absorption. Significant differences in the near-field intensity correlations between metallic and dielectric random systems are demonstrated.

DOI: 10.1103/PhysRevLett.94.226101 PACS numbers: 68.37.Uv, 42.25.Dd, 73.20.Mf, 77.55.+f

Spatial correlations of field and intensity have been widely studied in the context of electromagnetic (EM) wave propagation in disordered systems [1,2] and are indicative of the nature of wave transport in random media. In dielectric random systems, the enhancement of nonlocal intensity correlations due to localization effects has been theoretically [2] and experimentally investigated [3–6]. However, not much is known of near-field intensity correlations in disordered metallic systems, which may exhibit richer phenomena due to strong interactions between light and intrinsic material excitations—plasmons [7,8]. Nor is it clear the difference between correlation functions in metallic and dielectric random systems. In disordered metallic nanostructures, surface plasmon (SP) modes are governed by structural inhomogeneities and may be strongly localized [9]. Localization of surface plasmon polaritons (SPPs) has been observed in rough and semicontinuous metal films [10,11]. The near-field intensity distribution across a semicontinuous metal film near the ''percolation threshold'' is extremely inhomogeneous with giant local field maxima (hot spots) [9–12]. The hot spots not only vary in size by orders of magnitude from subwavelength to multiple wavelength (λ), but also vary strongly in intensity. These properties are very different from those in a dielectric random system where the speckle pattern is relatively more homogeneous with an average speckle size of the order of λ. Moreover, the accumulation and subsequent dissipation of EM energy in localized SP modes result in anomalous absorption in semicontinuous metal films [13–15]. These fundamental differences between metallic and dielectric random systems suggest that the near-field intensity correlation functions in these two systems can be dramatically different.

In this Letter, we present the first experimental study of near-field intensity correlations in semicontinuous metal films. The concentration p of metal particles on a dielectric surface is varied over a wide range to control the scattering strength. When p is far from the ''percolation threshold'' p_c, scattering is weak and the impinging light mostly excites extended SP modes. These propagating EM surface waves correlate the near-field intensity over large distances. When p is near p_c, substantial structural inhomogeneities result in strong scattering. The incident wave couples predominately to localized SP modes, and the near-field intensity correlation becomes short ranged. We compare the spatial intensity correlation functions in metal-dielectric and purely dielectric random systems to illustrate their differences.

Semicontinuous silver films on glass substrates were synthesized by pulsed laser deposition [12]. Transmission electron microscope (TEM) images reveal that the samples are composed of individual silver grains of average size about 20–30 nm. An increase in deposition time (surface concentration of silver) induces a structural transition from isolated metal grains ($p \lesssim 0.4$) to interconnected metal clusters ($p \sim 0.6$) and finally to a nearly continuous metal film with dielectric voids ($p \gtrsim 0.8$) [12]. For these samples, the percolation threshold was found to be at $p_c \approx 0.65$ from previous work [12]. The two-dimensional (2D) Fourier transforms of the structures, obtained from TEM micrographs, exhibit isotropic distributions in k space for all samples. The 2D structural correlation functions are also isotropic. The correlation radius, defined as the half width at half maximum (HWHM) of the structural correlation function, is close to the grain size. Its value is nearly constant for $p < p_c$ and increases slightly for $p > p_c$. In the near-field experiment, samples were illuminated by the evanescent field (in the total internal reflection geometry) of He-Ne lasers operating at 543 and 633 nm (p polarized). The local optical signal was collected by a tapered, uncoated optical fiber of tip radius $\sim$50 nm. The tip-to-sample distance, controlled by shear-force feedback, was $\sim$10 nm. The tip resolution was estimated to be $\sim$150 nm from the smallest features in the near-field images [12].

Figure 1 shows near-field scanning optical microscopy (NSOM) images for samples of $p = 0.36$, 0.45, 0.65, 0.75, 0.83 at a probe wavelength of 543 nm. The projection of the incident beam's k vector on the film plane ($x - y$ plane), $\mathbf{k}_\parallel$, is along the vertical y axis. At $p = 0.36$, there is a clear indication of interference fringes parallel to the horizontal x axis, which are weakened at $p = 0.45$ and completely lost at $p = 0.65$. The NSOM images at $p = 0.65$ exhibit inhomogeneous intensity distributions with hot spots of various sizes. The interference fringes start to reappear at $p = 0.75$ and are clearly visible at $p = 0.83$.

To identify the spatial frequencies or k vectors of excitations in a sample, 2D Fourier transforms of the near-field intensity distribution $I(x, y)$ were obtained. The beating of waves of different spatial frequencies results in intensity modulations, thus allowing the extraction of k vectors from the Fourier transform of the *intensity* distribution. In Fig. 1, the spatial Fourier spectra exhibit significant elongation of the k-vector distribution along the incident direction at low and high p, whereas the distribution is nearly isotropic at $p_c \approx 0.65$. This reflects changes in the scattering strength in the samples. At low densities of metal particles, both elastic and inelastic scattering are weak. Because of the small grain size, scattering by single metal particles occurs mainly in the forward and backward directions. Hence, the in-plane k vectors are predominately parallel or antiparallel to the incident wave vector $\mathbf{k}_\parallel$. As p increases, scattering becomes stronger and the impinging wave is more strongly scattered into other directions until the memory of the incident k vector is completely lost at p_c. With a further increase in p, the structure approaches that of a continuous metal film and scattering, now caused by dielectric voids, decreases again leading to a nonisotropic k distribution. Similar phenomena were also observed at the other probe wavelength of 633 nm. These data thus reveal that both weak and strong scattering regimes can be accessed by varying metal concentration.

From near-field images, the 2D correlation functions for near-field intensities were computed: $C(\Delta x, \Delta y) \equiv \langle \delta I(x, y) \delta I(x + \Delta x, y + \Delta y) \rangle$, where $\delta I(x, y) = [I(x, y) - \langle I(x, y) \rangle] / \langle I(x, y) \rangle$. Figure 2 shows the spatial dependence of $C(\Delta x, \Delta y)$ for samples with $p = 0.36$, 0.65, and 0.83 at $\lambda = 633$ nm. Fringes are present along the direction of the incident wave for $p = 0.36$ and 0.83, but disappear at $p = 0.65$. Figures 3 and 4 are plots of the correlation functions in the directions parallel and perpendicular to the incident wave vector $k_\parallel$, i.e., $C(0, \Delta y)$ and $C(\Delta x, 0)$. Along $k_\parallel$, $C(0, \Delta y)$ exhibits oscillatory behavior at $p = 0.36$ with a period of 870 nm. The oscillation is replaced by a monotonic decay at $p = 0.65$. The inset of Fig. 3, a log-linear plot of $C(0, \Delta y)$ at $p = 0.65$, indicates an exponential reduction in correlation for a Δy range of 50 nm to 0.9 μm (beyond 0.9 μm its value reduces to the noise level). At $p = 0.83$, the oscillations reappear with a smaller period of 690 nm. Oscillations are also observed for $p = 0.45$ and 0.75 (not shown here for figure clarity), but their amplitudes are damped quickly. The presence of oscillations in $C(0, \Delta y)$ indicates the excitation of propagating surface waves with well-defined wave vectors along the y axis. Note that oscillations have been reported in near-field correlations of thermal emission from a smooth surface of bulk metal, as a result of excitation of propagating SPPs [16]. Although all our samples are semicontinuous films, scattering due to structural inhomogeneities is rather weak at low and high p, as seen in Fig. 1. Hence, the incident wave is subjected to the effective medium properties, and coupled predominately to propagating EM modes. A detailed explanation of the propagating surface waves is given later. When p is near p_c, large structural inhomogeneities result in strong scattering. The disappearence of oscillations in the intensity correlation functions reveals the suppression of propagating surface waves with well-defined wave vectors. The impinging light is coupled mostly to localized SP modes. The local field fluctuations occur on the length scale of microscopic structures. Because of the wide range of structural scales in a semicontinuous metal film near p_c, no single length scale prevails. As a result, the intensity correlation function exhibits a monotonic decay. Therefore, the existence, suppression, and revival of the oscillations in the near-field intensity correlation function with increasing p reflect the variation in the coupling strength between the incident light and microscopic structural inhomogeneities of semicontinuous metal films.

It is clear from Fig. 4 that $C(\Delta x, 0)$ shows no oscillations at any metal concentration. Hence, there is no wave propa-

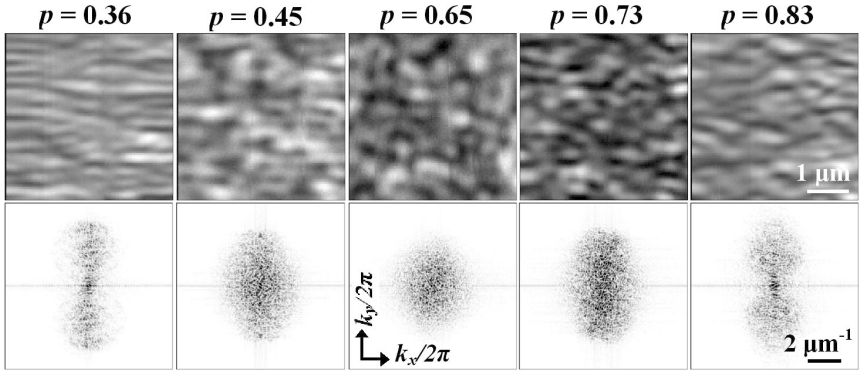

FIG. 1. The 4×4 μm^2 NSOM images (first row) and corresponding 2D Fourier spectra (second row) of semicontinuous silver films with different metal filling fractions p. The incident wave is along the vertical y axis. White areas correspond to higher intensities.

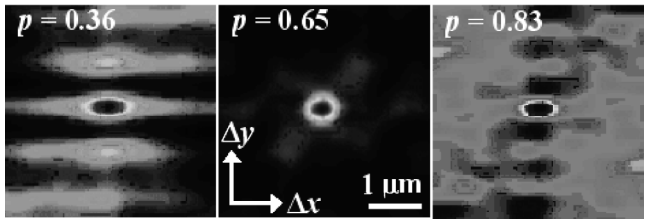

FIG. 2. The 2D intensity correlation functions $C(\Delta x, \Delta y)$ at $p = 0.36$, 0.65, and 0.83. The incident wave is along the y axis.

gation in the direction perpendicular to the incident wave vector. At $p = 0.36$, $C(\Delta x, 0)$ decreases gradually with Δx, but does not reduce to zero even at large Δx. The drop is much sharper at $p = 0.65$, and $C(\Delta x, 0)$ is almost zero when $\Delta x > 0.5$ μm. At $p = 0.83$, the decrease becomes gradual again and $C(\Delta x, 0)$ remains well above zero even for $\Delta x > 3$ μm. The long tail of $C(\Delta x, 0)$ suggests the existence of long-range correlation at low and high p, which results from a delocalized field. In the intermediate regime of metal concentration, the rapid decay of $C(\Delta x, 0)$ to zero indicates that the intensity correlation becomes short ranged because of strong scattering and anomalous absorption [13–15]. The correlation radius R_c [HWHM of $C(\Delta x, 0)$] allows a quantitative comparison between different samples and is plotted in the inset of Fig. 4 as a function of p for both probe wavelengths. R_c decreases from 500 nm at $p = 0.36$ to about 250 nm at $p = 0.45$, where it remains almost constant till $p = 0.75$. At $p = 0.83$, R_c increases to about 350 nm. This type of analysis was not attempted for $C(0, \Delta y)$ as the oscillations make it difficult to extract R_c. Nevertheless, the variation of correlation radius with p is consistent with the change in scattering strength exhibited in Fig. 1.

Near-field intensity correlations in disordered metal-dielectric structures appear to be very different from those in purely dielectric random media. In the latter, $C(\Delta \mathbf{r})$ is dominated by short-range correlation in the delocalization regime, whereas in the localization regime long-range correlation is greatly enhanced [2,3]. However, in the former, the intensity correlation becomes short ranged; i.e., $C(\Delta \mathbf{r})$ decays quickly to zero at $p \sim p_c$, where localization of SPPs is expected. In addition, $C(\Delta \mathbf{r})$ exhibits damped oscillations with a period of $\lambda/2$ in a dielectric random medium. In contrast, in a metallic random system, when scattering is weak, $C(\Delta \mathbf{r})$ oscillates with a period longer than $\lambda/2$ and the damping of the oscillations is much slower than in dielectric systems. As shown next, the oscillation period is determined by the characteristic length scales of collective excitations in the system.

Since a *single* propagating wave cannot induce oscillations in the *intensity* correlation function, the oscillations observed at low and high p indicate the existence of at least two propagating surface waves. To identify these waves, we calculated the wave vectors of the SPPs excited by the impinging light. At $p \gtrsim 0.8$, the system consists of a continuous network of silver clusters and can be treated as a continuous metal film with a random array of dielectric voids. SPPs may exist at both silver-air and silver-glass interfaces. The high metal concentration allows the use of the effective medium approximation to calculate the effective dielectric constant, which varies with p. The film permittivity is anisotropic: its value ε_e in the $x - y$ plane differs from ε_z in the z direction. At our probe wavelengths, $|\varepsilon_z| \gg |\varepsilon_e|$. Thus, the dispersion relation for SPP propagation ascribes the form

$$\varepsilon_d \times (1 - D\sqrt{-1 + x^2}\sqrt{-\varepsilon_e}) - \sqrt{x^2 - \varepsilon_d} \times (D\sqrt{-\varepsilon_e} + \sqrt{-1 + x^2}\varepsilon_e) = 0, \quad (1)$$

where $x = (c/\omega)k_{\mathrm{sp}}$, k_{sp} is the SPP wave vector, $D = \coth(\omega d\sqrt{-\varepsilon_e}/c)$, d is the film thickness, and ε_d is the dielectric constant of the glass substrate. Equation (1), a third-order equation in x^2, has only two physical solutions with values k_1 and k_2 for SPP at the silver-air ($z = -d/2$) and silver-glass ($z = d/2$) interfaces, respectively.

The conditions for the existence of SPPs in a semicontinuous metal film are as follows: (i) sufficiently small losses, i.e., $\mathrm{Re}[k_{1,2}] \gg \mathrm{Im}[k_{1,2}]$; (ii) $\mathrm{Re}[k_1] > \omega/c$,

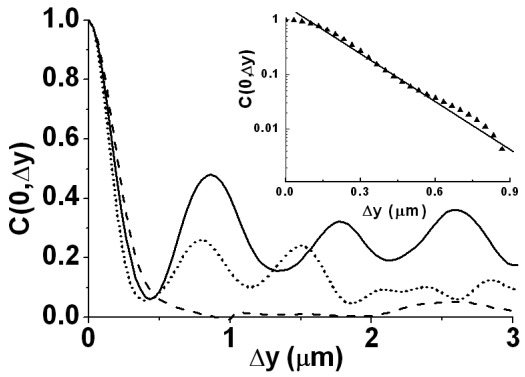

FIG. 3. $C(0, \Delta y)$ at $p = 0.36$ (solid line), 0.65 (dashed line), and 0.83 (dotted line) for incident wavelength 633 nm. Inset: log-linear plot of $C(0, \Delta y)$ at $p = 0.65$. For comparison, all $C(0, \Delta y)$ curves are divided by $C(0, 0)$.

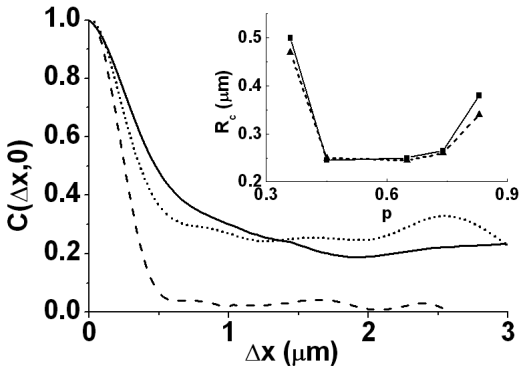

FIG. 4. $C(\Delta x, 0)$, again divided by $C(0, 0)$, at $p = 0.36$ (solid line), 0.65 (dashed line), and 0.83 (dotted line), for incident wavelength 633 nm. Inset: correlation radius R_c vs p for probe wavelengths at 633 nm (dashed line) and 543 nm (solid line).

$\mathrm{Re}[k_2] > \sqrt{\varepsilon_d}\omega/c$. These conditions can be fulfilled at sufficiently large metal concentrations ($p \gtrsim 0.8$). In a continuous silver film on glass ($p = 1$), SPPs cannot be excited at the silver-glass interface as the incident k vector is less than $\mathrm{Re}[k_2]$. However, for semicontinuous films used in the current experiment, SPPs are effectively excited due to the structural randomness and associated giant local field fluctuations [12]. The spatial beating between the fields of the two SPP waves results in a stationary intensity modulation with period $\lambda_s = 2\pi/|k_1 - k_2|$. At $p = 0.83$, we estimate $\lambda_s \simeq 640$ nm from Eq. (1) for incident light at 633 nm. λ_s should be equal to the oscillation period of the correlation function which, from Fig. 3, is about 690 nm and agrees well with the estimated value. Note that from our calculations, for $p < 0.7$, the total loss in the system, given by $\mathrm{Im}[k_2]$, is comparable to $\mathrm{Re}[k_2]$. Thus, $\mathrm{Im}[k_2]$ is large despite small intrinsic losses in the metal ($\mathrm{Im}[\varepsilon_m] \ll \mathrm{Re}[\varepsilon_m]$), which substantiates the anomalous absorption due to the localization of SPPs near p_c.

The oscillations of intensity correlation functions at low metal coverage $p \lesssim 0.4$ once more indicate the interference of two propagating waves. These oscillations cannot be explained solely by interference of the incident evanescent wave ($\lambda_\parallel = 2\pi/k_\parallel \approx 610$ nm) with the wave elastically backscattered by the metal particles, as the observed oscillation period (870 nm) is considerably larger than $\lambda_\parallel/2$. Therefore, there must exist another propagating wave with a different k vector. At $p \lesssim 0.4$, the sample consists of individually separated metal grains of nearly uniform shape. When collectively excited by incident light, these grains can be treated as oscillating dipoles with identical resonances and strong coupling between them [17,18]. For $p < p_c$, the semicontinuous silver film is in a dielectric state; its effective dielectric constant $\varepsilon_{\mathrm{eff}} = \varepsilon' + i\varepsilon''$ satisfies $\varepsilon' > 0$ and $\varepsilon' \gg \varepsilon''$. Using the Maxwell Garnet equation to estimate $\varepsilon_{\mathrm{eff}}$, we find that as p increases towards p_c, ε' increases and becomes significantly larger than the dielectric constants of the surrounding media (glass and air). A thin dielectric waveguide is thus formed at the surface of the glass substrate. The incident light excites mainly the lowest-order guided mode of this waveguide, leading to propagating surface waves. At $p = 0.36$ and $\lambda = 633$ nm, we estimate the wavelength of the lowest-order guided mode $\lambda_s = 383$ nm. The beating between the incident evanescent wave ($\lambda_\parallel \sim 610$ nm) and the propagating guided wave results in oscillations in the intensity correlation function with a period $\lambda_c \sim 1$ μm. From Fig. 3, the experimentally obtained $\lambda_c = 870$ nm is close to the estimated value.

Thus, the nature of the spatial intensity correlation functions show that as p increases, the semicontinuous metal film transitions from a dielectric waveguide at $p < p_c$ to a metallic waveguide at $p > p_c$. In between at $p \sim p_c$, the propagation of surface waves with well-defined wave vectors is greatly suppressed by strong scattering. At p below p_c, the intensity correlation function oscillates due to beating between the incident wave and propagating guided wave in the film. As p approaches p_c, scattering increases significantly and the oscillations in the correlation function disappear. We attribute this phenomenon to the localization of SPs. Finally, for p much above p_c, oscillations reappear in the correlation function due to beating between SPPs propagating along the top and bottom interfaces of the film.

Unlike dielectric random media, localized and delocalized modes are believed to coexist in metallic random systems [19]. Our experimental observations illustrate that at low and high metal coverages, delocalized modes dominate the transport, leading to the propagation of guided surface waves, while in the intermediate regime of metal content where structural inhomogeneities are substantial, localized modes take over, resulting in the localization of near-field energy. Both propagation and localization regimes have important applications. In the former, EM energy and information can be transferred over long distances, whereas the localization of EM fields in subwavelength scales can enhance various linear and nonlinear optical processes [9].

We thank A. L. Burin and A. A. Chabanov for discussions. This work is supported by NSF Grant No. DMR-0093949 and ARO Grant No. DAAD19-01-1-0682.

[1] *The Scattering and Localization of Classical Waves*, edited by P. Sheng (World Scientific, Singapore, 1990).
[2] R. Berkovits and S. Feng, Phys. Rep. **238**, 135 (1994); M. C. W. van Rossum and Th. M. Nieuwenhuizen, Rev. Mod. Phys. **71**, 313 (1999).
[3] P. Sebbah *et al.*, Phys. Rev. Lett. **88**, 123901 (2002).
[4] A. A. Chabanov *et al.*, Phys. Rev. Lett. **92**, 173901 (2004).
[5] V. Emiliani *et al.*, Phys. Rev. Lett. **90**, 250801 (2003).
[6] A. Apostol and A. Dogariu, Phys. Rev. Lett. **91**, 093901 (2003).
[7] J. A. Sanchez-Gil and M. Nieto-Vesperinas, Phys. Rev. B **45**, 8623 (1992).
[8] A. R. McGurn and A. A. Maradudin, Opt. Commun. **155**, 79 (1998).
[9] V. M. Shalaev, *Nonlinear Optics of Random Media* (Springer, Berlin, 2000); A. K. Sarychev and V. M. Shalaev, Phys. Rep. **335**, 275 (2000).
[10] S. I. Bozhevolnyi *et al.*, Phys. Rev. Lett. **89**, 186801 (2002); S. I. Bozhevolnyi *et al.*, Phys. Rev. Lett. **90**, 197403 (2003).
[11] D. P. Tsai *et al.*, Phys. Rev. Lett. **72**, 4149 (1994); S. Gresillon *et al.*, Phys. Rev. Lett. **82**, 4520 (1999).
[12] K. Seal *et al.*, Phys. Rev. B **67**, 35318 (2003).
[13] Y. Yagil *et al.*, Phys. Rev. B **46**, 2503 (1992).
[14] A. K. Sarychev *et al.*, Phys. Rev. B **51**, 5366 (1995).
[15] L. Zekri *et al.*, J. Phys. Condens. Matter **12**, 283 (2000).
[16] R. Carminati and J. Greffet, Phys. Rev. Lett. **82**, 1660 (1999).
[17] M. L. Brongersma *et al.*, Phys. Rev. B **62**, R16 356 (2000).
[18] A. L. Burin *et al.*, J. Opt. Soc. Am. B **21**, 121 (2004).
[19] M. I. Stockman *et al.*, Phys. Rev. Lett. **87**, 167401 (2001).